**The Fourth China-Japan-Korea Joint Symposium on Optimization of Structural and Mechanical Systems, Kunming, Nov. 6-9, 2006, China**

# Shape Optimization on Acoustic-Structure Interaction Problems

**Yoshiaki Hasegawa**[1], **Yasuhiko Kagiyama**[2], **Hideyuki Azegami**[1*]

[1] *Graduate School of Information Science, Nagoya University, 1 Furo-cho, Chikusa-ku, Nagoya 464-8601, Japan*

[*] *Corresponding author: azegami@is.nagoya-u.ac.jp*

[2] *Honda R & D Co. Tochigi R & D Center, 4630 Shimotakanezawa Haga-machi Haga-gun Tochigi 321-3393, Japan*

## Abstract

This paper presents a numerical method for solving nonparametric boundary shape optimization problems of acoustic-structure interaction problems. Weak form of the acoustic-structure interaction problem considering strong coupling is presented and used as state equations for the shape optimization problem. Sound pressure power integral in a sub-domain included in the acoustic field during frequencies of interest is chosen as an objective functional. Evaluation method of the shape gradient of the objective functional with respect to domain variation is derived theoretically by the adjoint variable method and the Lagrange multiplier method. Based on the shape gradient, a traction method proposed by Azegami and coworkers is applied for reshaping algorithm maintaining smoothness of the boundary shape. The validity of the solution is confirmed by numerical example for a box model made of linear elastic material surrounding a acoustic field.

**Key Words**: *Shape Optimization, Acoustic-Structure Interaction Problem, Shape gradient, Adjoint Variable Method, Traction Method*

## 1 Introduction

Numerical analysis of acoustic-structure interaction problems has come to perform more and more critical roles on noise and vibration problems. In recent years, parametric shape optimization problems for the acoustic-structure interaction problems have come to be solved using result of the numerical analysis. However, increase of design parameters brings about increase of computational cost. For high quality shape optimization with limited computational cost, non-parametric shape optimization is required.

In this paper, a numerical method for solving nonparametric boundary shape optimization problem for the acoustic-structure interaction problem is presented. In the next section, strong form of the acoustic-structure interaction problem and its weak form will be presented. A formulation of shape optimization problem for the acoustic-structure interaction problem selecting sound pressure power integral in a sub-domain included in the acoustic field during frequencies of interest as an objective functional and derivation of its shape gradient will be presented in Section 3. For reshaping algorithm using the shape gradient, the traction method proposed by Azegami and coworkers [1–7] will be applied to compensate lack of regularity of the shape gradient. To demonstrate the validity of the numerical method, numerical example for a box model made of linear elastic material surrounding a acoustic field will be analyzed.

## 2 Acoustic-Structure Interaction Problem

Considering structures such as vehicles, let an acoustic pressure field of $d = 2, 3$ dimensional domain $\Omega^{\mathrm{a}} \subset \mathbb{R}^d$ ($\mathbb{R}$ is the set of the real number), its boundary $\Gamma^{\mathrm{a}}$ be surrounded by a domain $\Omega^{\mathrm{s}} \subset \Omega^{\mathrm{fix}} \subset \mathbb{R}^d$, its boundary $\Gamma^{\mathrm{s}}$, that is interior of a fixed domain $\Omega^{\mathrm{fix}}$, of a linear elastic continuum as shown in Fig. 1. This means the whole boundary of the acoustic domain becomes interaction boundary with the elastic continuum ($\Gamma^{\mathrm{a}} \subset \Gamma^{\mathrm{s}}$). Let the linear elastic continuum deform with displacement $\boldsymbol{u}(\boldsymbol{x}, t) = \{u_i(\boldsymbol{x}, t)\}_{i=1}^{d}$ ($\boldsymbol{x} \in \Omega^{\mathrm{s}}$) by a non-zero boundary force $\boldsymbol{P}(\boldsymbol{x}, t)$ on a sub-boundary $\Gamma^P$ ($\boldsymbol{x} \in \Gamma^P$) at a time $t \in (-\infty, \infty)$ while restricting displacement $\boldsymbol{u} = \boldsymbol{0}$ on a sub-boundary $\Gamma_0$ and generate pressure $p(\boldsymbol{x}, t)$ ($\boldsymbol{x} \in \Omega^{\mathrm{a}}$) in the acoustic field. It is assumed during domain perturbations that the non-zero boundary force $\boldsymbol{P}(\boldsymbol{x}, t)$ is a fixed function defined in the fixed domain $\Omega^{\mathrm{fix}} \times (-\infty, \infty)$. In this paper, to obtain the symmetry of the weak form, a velocity potential

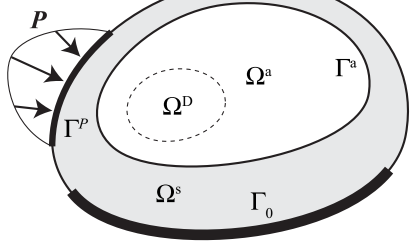


Fig. 1: Acoustic-structure interaction system

$\phi(\boldsymbol{x}, t)$ $(\boldsymbol{x} \in \Omega^{\mathrm{a}})$ is used instead of the pressure $p(\boldsymbol{x}, t)$ that is related with $p = \rho^{\mathrm{a}}\dot{\phi}$, where $\rho^{\mathrm{a}}$ is a density of the acoustic media.

The equations of motion for the acoustic-structure interaction system can be written as

$$\frac{\rho^{\mathrm{a}}}{c^2}\phi_{,tt} - \rho^{\mathrm{a}}\phi_{,ii} = 0 \qquad \text{in } \Omega^{\mathrm{a}} \tag{1}$$

$$\rho^{\mathrm{a}}\phi_{,i}n_i^{\mathrm{a}} + \rho^{\mathrm{a}}u_{i,t}n_i^{\mathrm{a}} = 0 \qquad \text{on } \Gamma^{\mathrm{a}} \tag{2}$$

$$\rho^{\mathrm{s}}u_{i,tt} - \sigma_{ij,j}(\boldsymbol{u}) = 0 \qquad \text{in } \Omega^{\mathrm{s}} \tag{3}$$

$$\sigma_{ij}(\boldsymbol{u})n_j^{\mathrm{s}} + \rho^{\mathrm{a}}\phi_{,t}n_i^{\mathrm{s}} = 0 \qquad \text{on } \Gamma^{\mathrm{a}} \tag{4}$$

$$u_i = 0 \qquad \text{on } \Gamma_0 \tag{5}$$

$$\sigma_{ij}(\boldsymbol{u})n_j^{\mathrm{s}} - P_i = 0 \qquad \text{on } \Gamma^P \tag{6}$$

where $c$ is a sound speed and $\rho^{\mathrm{s}}$ is a density of the linear elastic continuum. In this paper, the Einstein summation convention and the gradient notation $(\,\cdot\,)_{,i} \equiv \partial(\,\cdot\,)/\partial x_i$ and $(\,\cdot\,)_{,t} \equiv \partial(\,\cdot\,)/\partial t$ are used. Stress $\sigma_{ij}(\boldsymbol{u}) = C_{ijkl}\varepsilon_{kl}(\boldsymbol{u})$ is related with strain $\varepsilon_{ij}(\boldsymbol{u}) = (u_{i,j} + u_{j,i})/2$ and stiffness $\{C_{ijkl}\}_{i,j,k,l=1}^{d}$. The notation $\boldsymbol{n}^{\mathrm{m}} = \{n_i^{\mathrm{m}}\}_{i=1}^{d}$ denotes a outward normal vector on boundary of $\Omega^{\mathrm{m}}$.

Introducing an adjoint velocity potential $\varphi \in \Phi$ and an adjoint displacement $\boldsymbol{v} \in U$ and considering boundary conditions, the weak form of the equations of motion for $\phi \in \Phi$ and $\boldsymbol{u} \in U$ can be obtained as

$$\int_{-\infty}^{\infty} \left\{ a^{\mathrm{a}}(\phi, \varphi) + b^{\mathrm{a}}(\phi_{,tt}, \varphi) + c^{\mathrm{a}}(\varphi, \boldsymbol{u}_{,t}) + a^{\mathrm{s}}(\boldsymbol{u}, \boldsymbol{v}) + b^{\mathrm{s}}(\boldsymbol{u}_{,tt}, \boldsymbol{v}) + c^{\mathrm{s}}(\phi_{,t}, \boldsymbol{v}) \right\} \mathrm{d}t = \int_{-\infty}^{\infty} \langle \boldsymbol{P}, \boldsymbol{v} \rangle_{\Gamma^P} \, \mathrm{d}t \qquad \forall\varphi \in \Phi,\ \forall\boldsymbol{v} \in U \tag{7}$$

where the following definitions are used to simplify notation.

$$a^{\mathrm{a}}(\phi, \varphi) \equiv \int_{\Omega^{\mathrm{a}}} \rho^{\mathrm{a}}\phi_{,i}\varphi_{,i} \, \mathrm{d}\Omega \tag{8}$$

$$a^{\mathrm{s}}(\boldsymbol{u}, \boldsymbol{v}) \equiv \int_{\Omega^{\mathrm{s}}} \sigma_{ij}(\boldsymbol{u})\varepsilon_{ij}(\boldsymbol{v}) \, \mathrm{d}\Omega \tag{9}$$

$$b^{\mathrm{a}}(\phi, \varphi) \equiv \int_{\Omega^{\mathrm{a}}} \frac{\rho^{\mathrm{a}}}{c^2}\phi\varphi \, \mathrm{d}\Omega \tag{10}$$

$$b^{\mathrm{s}}(\boldsymbol{u}, \boldsymbol{v}) \equiv \int_{\Omega^{\mathrm{s}}} \rho^{\mathrm{s}}u_i v_i \, \mathrm{d}\Omega \tag{11}$$

$$c^{\mathrm{a}}(\varphi, \boldsymbol{u}) \equiv \int_{\Gamma^{\mathrm{a}}} \rho^{\mathrm{a}}\varphi u_i n_i^{\mathrm{a}} \, \mathrm{d}\Gamma \tag{12}$$

$$c^{\mathrm{s}}(\phi, \boldsymbol{v}) \equiv \int_{\Gamma^{\mathrm{a}}} \rho^{\mathrm{a}}\phi v_i n_i^{\mathrm{s}} \, \mathrm{d}\Gamma \tag{13}$$

$$\langle \boldsymbol{P}, \boldsymbol{v} \rangle_{\Gamma^P} \equiv \int_{\Gamma^P} P_i v_i \, \mathrm{d}\Gamma \tag{14}$$

$$\Phi \equiv \left\{ \varphi \in H^1\left(\Omega^{\mathrm{a}} \times \mathbb{R}\right) \right\} \tag{15}$$

$$U \equiv \left\{ \boldsymbol{v} \in \left(H^1\left(\Omega^{\mathrm{s}} \times \mathbb{R}\right)\right)^d \,\middle|\, \boldsymbol{v} = \boldsymbol{0} \text{ on } \Gamma_0 \right\} \tag{16}$$

Let $\hat{\boldsymbol{P}}(\boldsymbol{x},\omega)$ be the Fourier transform of $\boldsymbol{P}(\boldsymbol{x},t)$, that is

$$\boldsymbol{P}(\boldsymbol{x},t) = \int_{-\infty}^{\infty} \hat{\boldsymbol{P}}(\boldsymbol{x},\omega)\mathrm{e}^{\mathrm{j}\omega t}\,\mathrm{d}\left(\frac{\omega}{2\pi}\right) \tag{17}$$

where j is the imaginary unit. Similarly, $(\hat{\cdot})$ denotes the Fourier transform or the set of the Fourier transform. Substituting the relation of the inverse Fourier transform such as Eq. (17) into the weak form of Eq. (7), and considering damping effect with an acoustic damping coefficient $g^{\mathrm{a}}$ and a structural damping coefficient $g^{\mathrm{s}}$, the frequency domain representation of the weak form for $\hat{\phi} \in \hat{\Phi}$ and $\hat{\boldsymbol{u}} \in \hat{U}$ as

$$\int_{-\infty}^{\infty} A(\hat{\phi},\hat{\boldsymbol{u}},\hat{\varphi}^*,\hat{\boldsymbol{v}}^*)\,\mathrm{d}\omega = \int_{-\infty}^{\infty} \langle \hat{\boldsymbol{P}},\hat{\boldsymbol{v}}^*\rangle_{\Gamma^P}\,\mathrm{d}\omega \quad \forall\hat{\varphi}\in\hat{\Phi},\ \forall\hat{\boldsymbol{v}}\in\hat{U} \tag{18}$$

where $(\,\cdot\,)^*$ denotes the complex conjugate and

$$A(\hat{\phi},\hat{\boldsymbol{u}},\hat{\varphi}^*,\hat{\boldsymbol{v}}^*) \equiv (1+\mathrm{j}g^{\mathrm{a}})a^{\mathrm{a}}(\hat{\phi},\hat{\varphi}^*) - \omega^2 b^{\mathrm{a}}(\hat{\phi},\hat{\varphi}^*) + \mathrm{j}\omega c^{\mathrm{a}}(\hat{\varphi}^*,\hat{\boldsymbol{u}}) + (1+\mathrm{j}g^{\mathrm{s}})a^{\mathrm{s}}(\hat{\boldsymbol{u}},\hat{\boldsymbol{v}}^*) - \omega^2 b^{\mathrm{s}}(\hat{\boldsymbol{u}},\hat{\boldsymbol{v}}^*) + \mathrm{j}\omega c^{\mathrm{s}}(\hat{\phi},\hat{\boldsymbol{v}}^*). \tag{19}$$

It is noted that the left part of Eq. (18) is commutative for $(\hat{\phi},\hat{\boldsymbol{u}})$ and $(\hat{\varphi}^*,\hat{\boldsymbol{v}}^*)$, so the following symmetric matrix expression can be obtained using nodal vectors $\underline{\hat{\phi}}$, $\underline{\hat{\boldsymbol{u}}}$ and $\underline{\hat{\boldsymbol{P}}}$ for $\hat{\phi}$, $\hat{\boldsymbol{u}}$ and $\hat{\boldsymbol{P}}$ respectively.

$$\left(-\omega^2\begin{bmatrix}-\boldsymbol{M}^{\mathrm{a}} & \boldsymbol{0}\\ \boldsymbol{0} & \boldsymbol{M}^{\mathrm{s}}\end{bmatrix} + \mathrm{j}\omega\begin{bmatrix}\boldsymbol{0} & \boldsymbol{A}\\ \boldsymbol{A}^T & \boldsymbol{0}\end{bmatrix} + \begin{bmatrix}-\boldsymbol{K}^{\mathrm{a}} & \boldsymbol{0}\\ \boldsymbol{0} & \boldsymbol{K}^{\mathrm{s}}\end{bmatrix}\right)\begin{Bmatrix}\underline{\hat{\phi}}\\ \underline{\hat{\boldsymbol{u}}}\end{Bmatrix} = \begin{Bmatrix}\boldsymbol{0}\\ \underline{\hat{\boldsymbol{P}}}\end{Bmatrix} \tag{20}$$

This character will be used later to solve an adjoint problem by replacing only the right side of Eq. (20).

# 3 Sound Pressure Power Minimization Problem

In vehicle design, it is aimed to reduce a sound pressure power near the ears of passengers by modifying design of frame structure. An integral of the sound pressure power $\hat{p}\hat{p}^* = -\omega^2\rho^{\mathrm{a}2}\hat{\phi}\hat{\phi}^*$ in a sub-domain $\Omega^{\mathrm{D}} \subset \Omega^{\mathrm{a}}$, its boundary $\Gamma^{\mathrm{D}}$, as shown in Fig. 1, near the ears of passengers in the acoustic field during frequencies of interest $\omega_1 \le \omega \le \omega_2$ can be given by

$$J^{[0]}(\Omega^{\mathrm{s}},\hat{\phi}) \equiv \int_{\omega_1}^{\omega_2}\int_{\Omega^{\mathrm{D}}} \hat{p}\hat{p}^*\,\mathrm{d}\Omega\,\mathrm{d}\omega = \int_{\omega_1}^{\omega_2} -\omega^2 d(\hat{\phi},\hat{\phi}^*)\,\mathrm{d}\omega \tag{21}$$

where $d(\hat{\phi},\hat{\phi}^*)$ is defined as

$$d(\hat{\phi},\hat{\phi}^*) \equiv \int_{\Omega^{\mathrm{D}}} \rho^{\mathrm{a}2}\hat{\phi}\hat{\phi}^*\,\mathrm{d}\Omega. \tag{22}$$

A volume constraint of the linear elastic continuum not to exceed a given value $m_0$ can be written as

$$J^{[1]}(\Omega^{\mathrm{s}}) \equiv \int_{\Omega^{\mathrm{s}}} \mathrm{d}\Omega - m_0 \le 0. \tag{23}$$

Accordingly, applying the Lagrange multiplier method for the volume constraint using $\Lambda^{[1]}$ as the Lagrange multiplier, the sound pressure power minimization problem under the volume constraint can be written with the Lagrange multiplier form $L(\Omega^{\mathrm{s}},\hat{\phi},\Lambda^{[1]})$ as

$$\min_{\Omega^{\mathrm{s}}\subset\Omega^{\mathrm{fix}}}\ \max_{0\le\Lambda^{[1]}\in\mathbb{R}} \left\{L(\Omega^{\mathrm{s}},\hat{\phi},\Lambda^{[1]}) \equiv J^{[0]}(\Omega^{\mathrm{s}},\hat{\phi}) + \Lambda^{[1]}J^{[1]}(\Omega^{\mathrm{s}})\right\}$$
$$\text{such that } \int_{\omega_1}^{\omega_2} A(\hat{\phi},\hat{\boldsymbol{u}},\hat{\varphi}^*,\hat{\boldsymbol{v}}^*)\,\mathrm{d}\omega = \int_{\omega_1}^{\omega_2} \langle\hat{\boldsymbol{P}},\hat{\boldsymbol{v}}^*\rangle_{\Gamma^P}\,\mathrm{d}\omega \quad \forall\hat{\varphi}\in\hat{\Phi},\ \forall\hat{\boldsymbol{v}}\in\hat{U}. \tag{24}$$

The Kuhn-Tucker conditions of the shape optimization problem are obtained by

$$\dot{L}(\Omega^{\mathrm{s}},\hat{\phi},\Lambda^{[1]}) = 0 \tag{25}$$

$$\Lambda^{[1]}J^{[1]}(\Omega^{\mathrm{s}}) = 0 \tag{26}$$

$$J^{[1]}(\Omega^{\mathrm{s}}) \le 0 \tag{27}$$

$$\Lambda^{[1]} \ge 0 \tag{28}$$

where $\dot{L}(\Omega^{\mathrm{s}}, \hat{\phi}, \Lambda^{[1]})$ is the material derivative of $L(\Omega^{\mathrm{s}}, \hat{\phi}, \Lambda^{[1]})$ with respect to arbitrary velocity of domain variation $\boldsymbol{V} \in D$ given by

$$\dot{L}(\Omega^{\mathrm{s}}, \hat{\phi}, \Lambda^{[1]}) = \dot{J}^{[0]}(\Omega^{\mathrm{s}}, \hat{\phi}) + \Lambda^{[1]}\dot{J}^{[1]}(\Omega^{\mathrm{s}}) \tag{29}$$

$$\begin{aligned}\dot{J}^{[0]}(\Omega^{\mathrm{s}}, \hat{\phi}) &= -\omega^2\left\{\int_{\omega_1}^{\omega_2} d(\hat{\phi}', \hat{\phi}^*)\,\mathrm{d}\omega + \int_{\omega_1}^{\omega_2} d(\hat{\phi}, \hat{\phi}^{*\prime})\,\mathrm{d}\omega\right\} + \int_{\omega_1}^{\omega_2} \langle G^{[0]\mathrm{D}}\boldsymbol{n}^{\mathrm{D}}, \boldsymbol{V}\rangle_{\Gamma^{\mathrm{D}}}\,\mathrm{d}\omega \\ &= -\omega^2\left\{\int_{\omega_1}^{\omega_2} d(\hat{\phi}', \hat{\phi}^*)\,\mathrm{d}\omega + \int_{\omega_1}^{\omega_2} d(\hat{\phi}, \hat{\phi}^{*\prime})\,\mathrm{d}\omega\right\}\end{aligned} \tag{30}$$

$$\dot{J}^{[1]}(\Omega^{\mathrm{s}}) = \int_{\omega_1}^{\omega_2} \langle G^{[1]}\boldsymbol{n}^{\mathrm{s}}, \boldsymbol{V}\rangle_{\Gamma^{\mathrm{s}}}\,\mathrm{d}\omega \tag{31}$$

$$G^{[0]\mathrm{D}} = -\omega^2\rho^{\mathrm{a}2}\hat{\phi}\hat{\phi}^* \quad \text{on } \Gamma^{\mathrm{D}} \tag{32}$$

$$G^{[1]} = 1 \quad \text{on } \Gamma^{\mathrm{s}} \tag{33}$$

$$D = \left\{\boldsymbol{V} \in (C^{0,1}(\overline{\Omega^{\mathrm{a}} \cup \Omega^{\mathrm{s}}}))^d \;\middle|\; \boldsymbol{V} = \boldsymbol{0} \text{ in } \Omega^{\mathrm{D}}\right\}. \tag{34}$$

The notations $(\dot{\,\cdot\,})$ and $(\,\cdot\,)' = (\dot{\,\cdot\,}) - (\,\cdot\,)_{,i}V_i$ denote the material derivative and the shape derivative respectively [8].

Applying the adjoint variable method for the weak form in Eq. (24), a shape gradient of the objective functional can be obtained as follows. To take material derivative of the weak form with respect to arbitrary domain variation $\boldsymbol{V} \in D$ and to consider that $\hat{\phi}, \hat{\boldsymbol{u}}$ is the solution of the weak form lead to the following equation.

$$\int_{\omega_1}^{\omega_2} A(\hat{\phi}', \hat{\boldsymbol{u}}', \hat{\varphi}^*, \hat{\boldsymbol{v}}^*)\,\mathrm{d}\omega = \int_{\omega_1}^{\omega_2}\left(\langle G^{[0]\mathrm{a}}\boldsymbol{n}^{\mathrm{a}}, \boldsymbol{V}\rangle_{\Gamma^{\mathrm{a}}} + \langle G^{[0]\mathrm{s}}\boldsymbol{n}^{\mathrm{s}}, \boldsymbol{V}\rangle_{\Gamma^{\mathrm{s}}} + \langle G^{[0]P}\boldsymbol{n}^{\mathrm{s}}, \boldsymbol{V}\rangle_{\Gamma^{P}}\right)\mathrm{d}\omega$$
$$\hat{\varphi} \in \hat{\Phi},\ \hat{\boldsymbol{v}} \in \hat{U},\ \hat{\phi}' \in \hat{\Phi},\ \hat{\boldsymbol{u}}' \in \hat{U},\ \forall \boldsymbol{V} \in D \tag{35}$$

$$G^{[0]\mathrm{a}} = -(1 + \mathrm{j}g^{\mathrm{a}})\rho^{\mathrm{a}}\hat{\phi}_{,i}\hat{\varphi}^*_{,i} + \omega^2\frac{\rho^{\mathrm{a}}}{c^2}\hat{\phi}\hat{\varphi}^* - \mathrm{j}\omega\left\{\rho^{\mathrm{a}}\left(\hat{\varphi}^*\hat{u}_i - \hat{\phi}\hat{v}^*_i\right)n^{\mathrm{a}}_i\right\}_{,j} n^{\mathrm{a}}_j - \mathrm{j}\omega\rho^{\mathrm{a}}\left(\hat{\varphi}^*\hat{u}_i - \hat{\phi}\hat{v}^*_i\right)n^{\mathrm{a}}_i\kappa^{\mathrm{a}} \quad \text{on } \Gamma^{\mathrm{a}} \tag{36}$$

$$G^{[0]\mathrm{s}} = -(1 + \mathrm{j}g^{\mathrm{s}})\sigma_{ij}(\hat{\boldsymbol{u}})\varepsilon_{ij}(\hat{\boldsymbol{v}}^*) + \omega^2\rho^{\mathrm{s}}\hat{u}_i\hat{v}^*_i \quad \text{on } \Gamma^{\mathrm{s}} \tag{37}$$

$$G^{[0]P} = (\hat{P}_i\hat{v}^*_i)_{,j}n^{\mathrm{s}}_j + \hat{P}_i\hat{v}^*_i\kappa^{\mathrm{s}} \quad \text{on } \Gamma^{P} \tag{38}$$

where $\kappa^{\mathrm{m}}$ is the $d-1$ times of the mean curvature on the boundary of $\Omega^{\mathrm{m}}$. Here, let us define a adjoint problem with a weak form for $\hat{\varphi} \in \hat{\Phi}$ and $\hat{\boldsymbol{v}} \in \hat{U}$ by

$$\int_{\omega_1}^{\omega_2} A(\hat{\phi}', \hat{\boldsymbol{u}}', \hat{\varphi}^*, \hat{\boldsymbol{v}}^*)\,\mathrm{d}\omega = -\omega^2\left\{\int_{\omega_1}^{\omega_2} d(\hat{\phi}', \hat{\phi}^*)\,\mathrm{d}\omega + \int_{\omega_1}^{\omega_2} d(\hat{\phi}, \hat{\phi}^{*\prime})\,\mathrm{d}\omega\right\} \quad \forall\hat{\phi}' \in \hat{\Phi},\ \forall\hat{\boldsymbol{u}}' \in \hat{U}. \tag{39}$$

Using the solution of the adjoint problem $\hat{\varphi}, \hat{\boldsymbol{v}}$ and noting that the right side of Eq (30) coincides with the right side of Eq. (39) and the left side of Eq. (39) coincides with the left side of Eq. (35), the following relation can be obtained.

$$\begin{aligned}\dot{J}^{[0]}(\Omega^{\mathrm{s}}, \hat{\phi}) &= \int_{\omega_1}^{\omega_2}\left(\langle G^{[0]\mathrm{a}}\boldsymbol{n}^{\mathrm{a}}, \boldsymbol{V}\rangle_{\Gamma^{\mathrm{a}}} + \langle G^{[0]\mathrm{s}}\boldsymbol{n}^{\mathrm{s}}, \boldsymbol{V}\rangle_{\Gamma^{\mathrm{s}}} + \langle G^{[0]P}\boldsymbol{n}^{\mathrm{s}}, \boldsymbol{V}\rangle_{\Gamma^{P}}\right)\mathrm{d}\omega \\ &\equiv \int_{\omega_1}^{\omega_2}\langle G^{[0]}\boldsymbol{n}^{\mathrm{s}}, \boldsymbol{V}\rangle_{\Gamma^{\mathrm{s}}}\,\mathrm{d}\omega\end{aligned} \tag{40}$$

Based on the results obtained above, the shape gradients for $J^{[0]}$ and $J^{[1]}$ were obtained as $G^{[0]}\boldsymbol{n}^{\mathrm{s}}$ in Eq. (40), which can be calculated by Eqs. (36) to (38) using the solutions of the original and adjoint problems, and $G^{[1]}\boldsymbol{n}^{\mathrm{s}} = \boldsymbol{n}^{\mathrm{s}}$ in Eq. (31) respectively. The adjoint problem given by Eq. (39) can be solved by the finite-element method using Eq. (20) replacing $(\underline{\hat{\phi}}, \underline{\hat{\boldsymbol{u}}})$ by $(\underline{\hat{\varphi}^*}, \underline{\hat{\boldsymbol{v}}^*})$ and the right side by the nodal vector of the right side of Eq. (39).

# 4 Traction Method

Since the shape gradients were obtained, the concept of the gradient method can be applicable to reshaping algorithm. However, because of the lack of regularity of the shape gradient $G^{[0]}\boldsymbol{n}^{\mathrm{s}}$ [9], moving boundary nodes of a finite-element model in proportion to an evaluated value of $-G^{[0]}\boldsymbol{n}^{\mathrm{s}}$ by the normal finite-element method falls into wavy shapes. To

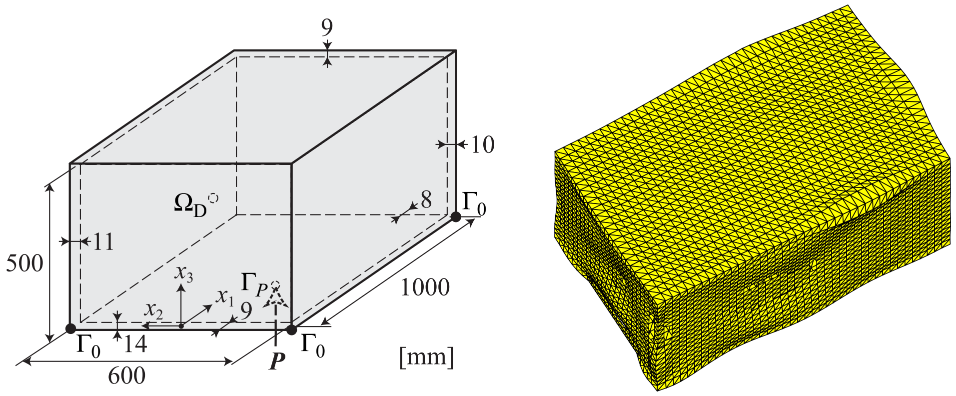


(a) Initial shape

(b) Optimized shape
(Domain variation was extended 10 times)

Fig. 2: Shape optimization of box model

compensate for the lack of smoothness of the shape gradient, a smoothing gradient method called traction method has been developed by Azegami and coworkers by applying the gradient method in Hilbert space [1–5].

In the traction method, domain variation that minimizes a functional is obtained as a solution to a boundary value problem of a linear elastic continuum defined in the design domain and loaded with traction in proportion to the negative shape gradient on the design boundary. In other words, the negative shape gradient is used for the Neumann condition on the design boundary. An improved version of the traction method using the Robin condition instead of the Neumann condition was proposed by Azegami and Takeuch [7].

A precise algorithm of the traction method including the determination of the Lagrange multipliers was presented in the previous paper [6].

# 5 Numerical example

A box model made of linear elastic material surrounding a acoustic field as shown in Fig. 2 (a) was analyzed. The sizes of the box shown in Fig. 2 (a) indicate between the centers of the thicknesses. The displacement was constrained at the four corner points of the bottom plane for $\Gamma_0$ through springs of spring constants 49, 49, and 98[N/mm] in $x_1$, $x_2$ and $x_3$ directions respectively. The boundary force $\boldsymbol{P}$ was assumed as a nodal force at a node (225.3253, −174.709, −7.0) (unit:[mm]) of the finite element model for $\Gamma^P$, in which the origin of the coordinate axes located in the front plane and at the center thickness of the bottom plate. The sound pressure power was evaluated between 90 to 225 [Hz] at a node (198.7542, 158.9309, 276.3181) (unit:[mm]) of the finite element model for $\Omega^{\mathrm{D}}$. The shape variation was constrained on $\Gamma_0$, $\Gamma^P$, and $\Gamma^{\mathrm{a}}$. Values of sound speed 340 m/s, density of air and elastic continuum 1.178[kg/m$^3$] and 7.80×10$^3$[kg/m$^3$], Young's modulus 205.8[GPa], Poisson's ratio 0.33, structural viscous damping factor 0.06 and sound viscous damping factor 0.12.

In this study, MSC.NASTRAN was used to solve the acoustic-structure interaction problem and the adjoint problem. A program for shape optimization was developed using the libraries developed by Azegami laboratory.

Figure 3 shows the variation of the frequency response of the pressure norm $\|\hat{p}\|_{L^2(\Omega^{\mathrm{D}})}/\|\hat{\boldsymbol{P}}\|_{(L^2(\Gamma^P))^3}$ at the initial and the optimized models. It was confirmed the decrease in the sound pressure norm between 90 to 225[Hz].

# 6 Conclusions

Shape optimization problem of acoustic-structure interaction problem was formulated as a non-parametric shape optimization problem. Shape gradient of the sound pressure power integral in a sub-domain in the acoustic field during frequencies of interest was derived theoretically. Based on the shape gradient, solution of the shape optimization problem

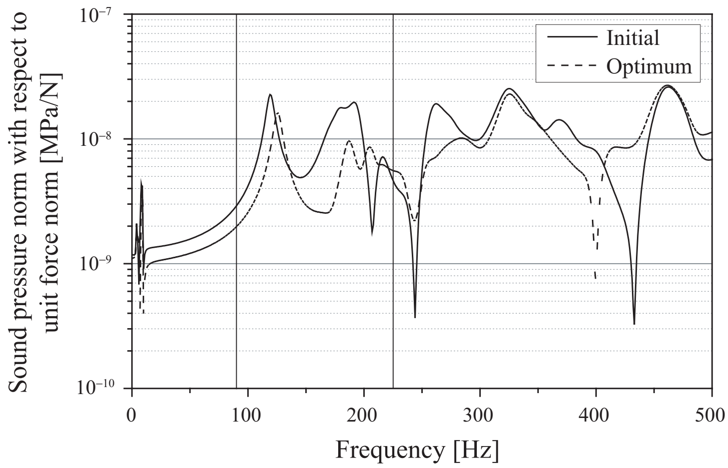


Fig. 3: Frequency response of sound pressure norm

using the traction method was proposed. The validity of the solution was confirmed by numerical example for a box model made of linear elastic material surrounding an acoustic field.

# References

[1] H. Azegami. A solution to domain optimization problems. *Trans. of Jpn. Soc. of Mech. Engs., Ser. A*, 60:1479–1486, 1994. (in Japanese).

[2] H. Azegami, M. Shimoda, E. Katamine, and Z. C. Wu. A domain optimization technique for elliptic boundary value problems. In S. Hernandez, M. El-Sayed, and C. A. Brebbia, editors, *Computer Aided Optimization Design of Structures IV, Structural Optimization*, pages 51–58. Computational Mechanics Publications, Southampton, 1995.

[3] H. Azegami and Z. C. Wu. Domain optimization analysis in linear elastic problems (approach using traction method). *JSME International Journal, Ser. A*, 39:272– 278, 1996.

[4] H. Azegami, S. Kaizu, M. Shimoda, and E. Katamine. Irregularity of shape optimization problems and an improvement technique. In S. Hernandez and C. A. Brebbia, editors, *Computer Aided Optimization Design of Structures V*, pages 309–326. Computational Mechanics Publications, Southampton, 1997.

[5] H. Azegami. Solution to boundary shape identification problems in elliptic boundary value problems using shape derivatives. In M. Tanaka and G.S. Dulikravich, editors, *Inverse Problems in Engineering Mechanics II*, pages 277–284. Elsevier, Tokyo, 2000.

[6] H. Azegami. Solution to boundary shape optimization problems. In C. A. Brebbia and W. P. de Wilde, editors, *High Performance Structures and Materials II*, pages 589–598. WIT Press, Southampton, UK, 2004.

[7] H. Azegami and K. Takeuchi. A smoothing method for shape optimization: traction method using the Robin condition. *International Journal of Computational Methods*, 3(1):21–33, 2006.

[8] J. Sokolowski and J. P. Zolésio. *Introduction to Shape Optimization: Shape Sensitivity Analysis*. Springer–Verlag, New York, 1991.

[9] S. Kaizu and H. Azegami. Optimal shape problems and traction method. *Transactions of the Japan Society for Industrial and Applied Mathematics*, 16(3):(in press), 2006. (in Japanese).